INTERNATIONAL JOURNAL OF
NUMERICAL ANALYSIS AND MODELING
Volume 8, Number 3, Pages 391–409

ELEMENT-BY-ELEMENT POST-PROCESSING OF DISCONTINUOUS GALERKIN METHODS FOR NAGHDI ARCHES

FATIH CELIKER, LI FAN, AND ZHIMIN ZHANG

Abstract. In this paper, we consider discontinuous Galerkin approximations to the solution of Naghdi arches and show how to post-process them in an element-by-element fashion to obtain a far better approximation. Indeed, we prove that, if polynomials of degree k are used, the post-processed approximation converges with order $2k+1$ in the L^2-norm *throughout the domain*. This has to be contrasted with the fact that before post-processing, the approximation converges with order $k+1$ only. Moreover, we show that this superconvergence property does not deteriorate as the thickness of the arch becomes extremely small. Numerical experiments verifying the above-mentioned theoretical results are displayed.

Key words. Post-processing, superconvergence, discontinuous Galerkin methods, Naghdi arches

1. Introduction

In [5], a family of discontinuous Galerkin (DG) methods for a Naghdi-type arch model was introduced as a step towards the difficult goal of devising locking-free DG methods for shells. They have proved that the approximation converges with order $k+1$ when polynomials of degree k are used. In this paper, we construct an element-by-element post-processing that converges remarkably faster.

This post-processing is based on the fact that a superconvergence phenomenon takes place at the nodes of the mesh. Indeed, the numerical traces of the DG method converge to the nodal values of the exact solution with order $2k+1$ when polynomials of degree k are used to compute the DG approximation, see [5]. The main goal of this paper is to exploit this phenomenon to post-process the DG solution element-by-element and obtain a better solution which superconverges to the exact solution with order $2k+1$ in the L^2-norm throughout the domain rather than at merely some isolated points of the mesh.

A similar superconvergent post-processing result has been proved for DG methods for convection-diffusion problems in [3]. Based on the superconvergence result proved therein, Cockburn and Ichikawa [7] devised a post-processing for the approximation of linear functionals which is superconvergent of order $4k+1$. In [2] Celiker and Cockburn designed a post-processing for DG methods for Timoshenko beams which is superconvergent of order $2k+1$ in the L^∞-norm throughout the computational domain. This result was based on the numerical observation that the numerical traces of the DG approximation for Timoshenko beams are also superconvergent of order $2k+1$ at the nodes of the mesh. Shortly later, the superconvergence of the numerical traces was put on a firm mathematical ground in [4].

As we will describe below, the Timoshenko beam model can be viewed as a special case of the Naghdi arch model where the beam is considered as an arch with zero curvature. The post-processing we display in this paper is thus inspired

Received by the editors October 30, 2010 and, in revised form, November 11, 2010.
2000 *Mathematics Subject Classification.* 65M60, 65N30, 35L65.
The third author was partially supported by the National Science Foundation (Grant DMS-0612908).

by the one introduced in [2]. Despite this close similarity, the coupling of some of the unknowns in the Naghdi arch model renders both the post-processing and its error analysis more involved. This is especially the case for the latter because it requires the analysis of a linear system of initial value problems whose solution is approximated by using approximate data. This is the main reason why we prove an L^2-error estimate for the post-processed approximation unlike the L^∞-error estimate for the Timoshenko beam post-processing. Notwithstanding, it is possible to prove an L^∞-error estimate at the expense of requiring high order regularity, following, for example, [11, 17].

Next, we describe the Naghdi arch model . A dimensionless form of this model can be written as a system of first order differential equations:

$$
\begin{aligned}
&(1a) \qquad & w' &+ \theta & &+ \kappa u &= d^2 T,\\
&(1b) \qquad & u' & & &- \kappa w &= d^2 N,\\
&(1c) \qquad & \theta' &+ \kappa(u' - \kappa w) & & &= M,\\
&(1d) \qquad & M' & & & &= T,\\
&(1e) \qquad & N' &+ (\kappa M)' & &- \kappa T &= p,\\
&(1f) \qquad & T' &+ \kappa^2 M & &+ \kappa N &= q,
\end{aligned}
$$

defined on $\Omega = (0, 1)$. For the simplicity of our notation we have assumed that the model is non-dimensionalized in a way that all the material properties including the Young's modulus, shear modulus, moment of inertia, and the length of the arch are scaled to be equal to one. However, all the results in this paper can be generalized to the case in which they are non-constant functions. The small parameter $d > 0$ represents the dimensionless thickness of the arch. The function κ is x-dependent, and $\kappa(x)$ is the curvature of the middle curve of the arch at the point of coordinate x. When κ is constantly valued, the arch is circular. A straight beam could be viewed as a special arch with $\kappa \equiv 0$, in which case (1) decouples to the Timoshenko beam bending model. The functions p and q are the tangential and transverse resultant loads, respectively. Similarly, a displacement vector of a point of the middle curve is decomposed to its tangent component u and normal component w. The remaining unknowns are the rotation of the normal fibers, θ, the bending moment, M, the scaled membrane stress, N, and the scaled shear stress, T. In Figure 1 we display some of the characteristics of a typical arch. The parametrization is indicated by

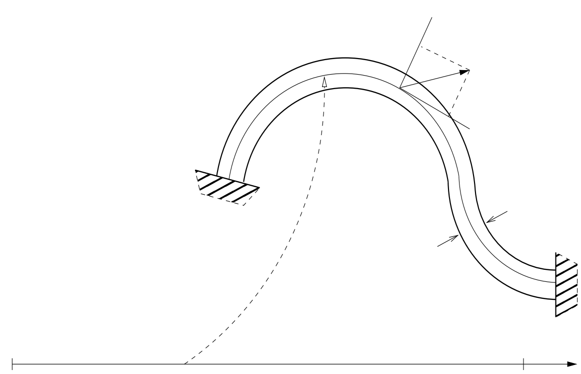

Figure 1. Cross section of an arch clamped at both ends, and arc length parametrization of its middle curve.

the mapping that maps $P \in [0,1]$ to P' on the middle curve. The x coordinate of P is equal to the arc length of the portion of the middle curve from its left end to P'.

Notwithstanding the fact that (1) constitutes a starting point from which one could derive DG methods, in [5] we derived the DG methods based on a slightly simplified model that has, as approximations to the elasticity theory, the same accuracy as the Naghdi model. It has been shown that the terms $\kappa(u' - \kappa w)$ in (1c), $(\kappa M)'$ in (1d), and $\kappa^2 N$ in (1f) can be neglected without significantly affecting the accuracy of the model. We will embrace these simplifications and henceforth work with the following governing equations

$$\begin{aligned}
&\text{(2a)} && w' + \theta + \kappa u = d^2 T,\\
&\text{(2b)} && u' - \kappa w = d^2 N,\\
&\text{(2c)} && \theta' = M,\\
&\text{(2d)} && M' = T,\\
&\text{(2e)} && N' - \kappa T = p,\\
&\text{(2f)} && T' + \kappa N = q.
\end{aligned}$$

in $\Omega := (0,1)$. To complete the model and ensure the existence and uniqueness of its solution we must impose suitable boundary conditions; we take, for example, the following clamped boundary conditions:

$$\text{(3)} \qquad \begin{aligned} w(0) &= w_0, & u(0) &= u_0, & \theta(0) &= \theta_0,\\ w(1) &= w_1, & u(1) &= u_1, & \theta(1) &= \theta_1. \end{aligned}$$

The rest of the paper is organized as follows. In Section 2, we recall the DG methods for Naghdi arches and sufficient conditions for the existence and uniqueness of their approximate solution. In Section 3, we describe the post-processing of the DG solution, and in Section 4 we prove the superconvergence of the post-processed approximation. Numerical results verifying our theoretical findings are presented in Section 5. We end in Section 6 with some concluding remarks.

2. The DG methods

To define the DG methods, we begin by partitioning the computational domain into intervals. Given the set of nodes

$$\mathcal{E}_h := \{x_0, x_1, \ldots, x_{\mathcal{N}}\},$$

where $0 = x_0 < x_1 < \cdots < x_{\mathcal{N}-1} < x_{\mathcal{N}} = 1$, we set

$$I_j := (x_{j-1}, x_j), \qquad h_j := x_j - x_{j-1}, \quad \text{and} \quad h := \max_{1 \le j \le \mathcal{N}}.$$

We also set

$$\Omega_h := \cup_{j=1}^{\mathcal{N}} I_j,$$

and we write

$$(f,g)_{\Omega_h} := \sum_{j=1}^{\mathcal{N}} \int_{I_j} fg \quad \text{and} \quad \langle R, [\![f]\!] \rangle_{\mathcal{E}_h} := \sum_{j=0}^{\mathcal{N}} R(x_j) [\![f]\!](x_j).$$

Here, R is any function defined on the set of nodes $\mathcal{E}_h$ and $[\![f]\!]$ is the *jump* of the function f across the nodes which is defined as follows

$$[\![f]\!](x_j) = \begin{cases} -f(0^+) & \text{for } j = 0, \\ f(x_j^-) - f(x_j^+) & \text{for } 0 < j < \mathcal{N}, \\ f(1^-) & \text{for } j = \mathcal{N}, \end{cases}$$

where $f(x_j^{\pm}) := \lim_{\epsilon \downarrow 0} f(x_j \pm \epsilon)$.

The approximate solution

$$\boldsymbol{\varphi}_h := (T_h, N_h, M_h, \theta_h, u_h, w_h)$$

given by the DG method is sought in the finite dimensional space $[V_h^k]^6$ where

$$V_h^k := \{v : \Omega_h \mapsto \mathbb{R} : \quad v|_{I_j} \in P^k(I_j), j = 1, \dots, \mathcal{N}\},$$

and $P^k(K)$ is the set of all polynomials on K of degree not exceeding k. It is determined by requiring that

$$\begin{aligned}
&\text{(4a)} && -(w_h, v_1')_{\Omega_h} + \langle \widehat{w}_h, [\![v_1]\!]\rangle_{\mathcal{E}_h} + (\theta_h, v_1)_{\Omega_h} + (\kappa\, u_h, v_1)_{\Omega_h} = d^2(T_h, v_1)_{\Omega_h} \\
&\text{(4b)} && -(u_h, v_2')_{\Omega_h} + \langle \widehat{u}_h, [\![v_2]\!]\rangle_{\mathcal{E}_h} - (\kappa\, w_h, v_2)_{\Omega_h} = d^2(N_h, v_2)_{\Omega_h} \\
&\text{(4c)} && -(\theta_h, v_3')_{\Omega_h} + \langle \widehat{\theta}_h, [\![v_3]\!]\rangle_{\mathcal{E}_h} = (M_h, v_3)_{\Omega_h} \\
&\text{(4d)} && -(M_h, v_4')_{\Omega_h} + \langle \widehat{M}_h, [\![v_4]\!]\rangle_{\mathcal{E}_h} = (T_h, v_4)_{\Omega_h} \\
&\text{(4e)} && -(N_h, v_5')_{\Omega_h} + \langle \widehat{N}_h, [\![v_5]\!]\rangle_{\mathcal{E}_h} - (\kappa\, T_h, v_5)_{\Omega_h} = (p, v_5)_{\Omega_h} \\
&\text{(4f)} && -(T_h, v_6')_{\Omega_h} + \langle \widehat{T}_h, [\![v_6]\!]\rangle_{\mathcal{E}_h} + (\kappa\, N_h, v_6)_{\Omega_h} = (q, v_6)_{\Omega_h}
\end{aligned}$$

hold for all $v_i \in V_h^k$ for $i = 1, \dots, 6$.

To complete the definition of the method, we have to define the numerical traces

$$\widehat{\boldsymbol{\varphi}}_h := (\widehat{T}_h, \widehat{N}_h, \widehat{M}_h, \widehat{\theta}_h, \widehat{u}_h, \widehat{w}_h)$$

at the nodes. We assume that the general form of these traces is as follows. For an interior node $x_j \in \mathcal{E}_h^\circ := \{x_1, x_2, \dots, x_{\mathcal{N}-1}\}$, we take

(5)
$$\begin{aligned}
\widehat{w}_h &= \{\!\{ w_h \}\!\} + C_{11}[\![w_h]\!] + C_{12}[\![u_h]\!] + C_{13}[\![\theta_h]\!] + C_{14}[\![M_h]\!] + C_{15}[\![N_h]\!] + C_{16}[\![T_h]\!], \\
\widehat{u}_h &= \{\!\{ u_h \}\!\} + C_{21}[\![w_h]\!] + C_{22}[\![u_h]\!] + C_{23}[\![\theta_h]\!] + C_{24}[\![M_h]\!] + C_{25}[\![N_h]\!] + C_{26}[\![T_h]\!], \\
\widehat{\theta}_h &= \{\!\{ \theta_h \}\!\} + C_{31}[\![w_h]\!] + C_{32}[\![u_h]\!] + C_{33}[\![\theta_h]\!] + C_{34}[\![M_h]\!] + C_{35}[\![N_h]\!] + C_{36}[\![T_h]\!], \\
\widehat{M}_h &= \{\!\{ M_h \}\!\} + C_{41}[\![w_h]\!] + C_{42}[\![u_h]\!] + C_{43}[\![\theta_h]\!] + C_{44}[\![M_h]\!] + C_{45}[\![N_h]\!] + C_{46}[\![T_h]\!], \\
\widehat{N}_h &= \{\!\{ N_h \}\!\} + C_{51}[\![w_h]\!] + C_{52}[\![u_h]\!] + C_{53}[\![\theta_h]\!] + C_{54}[\![M_h]\!] + C_{55}[\![N_h]\!] + C_{56}[\![T_h]\!], \\
\widehat{T}_h &= \{\!\{ T_h \}\!\} + C_{61}[\![w_h]\!] + C_{62}[\![u_h]\!] + C_{63}[\![\theta_h]\!] + C_{64}[\![M_h]\!] + C_{65}[\![N_h]\!] + C_{66}[\![T_h]\!],
\end{aligned}$$

where $\{\!\{f\}\!\}(x_j) := \frac{1}{2}(f(x_j^-) + f(x_j^+))$. At $x = 0$, we take

$$\begin{aligned}
\widehat{w}_h &= w_0, \\
\widehat{u}_h &= u_0, \\
\widehat{\theta}_h &= \theta_0, \\
\widehat{M}_h &= M_h^+ \quad + C_{41}(w_0 - w_h^+) + C_{42}(u_0 - u_h^+) + C_{43}(\theta_0 - \theta_h^+), \\
\widehat{N}_h &= N_h^+ \quad + C_{51}(w_0 - w_h^+) + C_{52}(u_0 - u_h^+) + C_{53}(\theta_0 - \theta_h^+), \\
\widehat{T}_h &= T_h^+ \quad + C_{61}(w_0 - w_h^+) + C_{62}(u_0 - u_h^+) + C_{63}(\theta_0 - \theta_h^+),
\end{aligned} \tag{6}$$

and at $x = 1$,

$$
\begin{aligned}
\widehat{w}_h &= w_1, \\
\widehat{u}_h &= u_1, \\
\widehat{\theta}_h &= \theta_1, \\
\widehat{M}_h &= M_h^- \quad + C_{41}(w_h^- - w_1) + C_{42}(u_h^- - u_1) + C_{43}(\theta_h^- - \theta_1), \\
\widehat{N}_h &= N_h^- \quad + C_{51}(w_h^- - w_1) + C_{52}(u_h^- - u_1) + C_{53}(\theta_h^- - \theta_1), \\
\widehat{T}_h &= T_h^- \quad + C_{61}(w_h^- - w_1) + C_{62}(u_h^- - u_1) + C_{63}(\theta_h^- - \theta_1).
\end{aligned} \tag{7}
$$

This completes the definition of the DG methods.

Note how the boundary conditions are incorporated into the method through the definition of the numerical traces at the border. Note also that the functions C_{ij} defining the numerical traces are not necessarily constant on $\mathcal{E}_h$, and can have different values at different nodes. Of course, not every choice of the C_{ij} leads to a well defined method. Conditions on these functions which ensure the existence and uniqueness of the DG solution can be found in [5]. We quote it here for the sake of completeness.

Theorem 2.1. *Consider the DG method defined by the weak formulation* (4) *and the numerical traces given by* (5)–(7)*. Suppose that at* all *nodes $e \in \mathcal{E}_h$ we have*

$$
\begin{aligned}
&C_{66} = -C_{11}, \quad C_{56} = -C_{12}, \quad C_{46} = -C_{13}, \quad C_{36} = -C_{14}, \quad C_{26} = -C_{15}, \\
&C_{65} = -C_{21}, \quad C_{55} = -C_{22}, \quad C_{45} = -C_{23}, \quad C_{35} = -C_{24}, \\
&C_{64} = -C_{31}, \quad C_{54} = -C_{32}, \quad C_{44} = -C_{33}, \\
&C_{63} = -C_{41}, \quad C_{53} = -C_{42}, \\
&C_{62} = -C_{51},
\end{aligned} \tag{8}
$$

that

$$
-C_{16},\ -C_{25},\ -C_{34} \geq 0, \tag{9}
$$

and that

$$
-C_{43},\ -C_{52},\ -C_{61} > 0. \tag{10}
$$

Then the method has a unique solution provided that

$$
h_j \leq \frac{1}{2\|\kappa - \overline{\kappa}_j\|_{L^\infty(I_j)}} \tag{11}
$$

on the elements I_j where κ is not identically equal to a constant. Here $\overline{\kappa}_j$ denotes the average value of κ on I_j.

Observe that the condition (8) shows that not all the C_{ij}'s are *independent*. More explicitly, 15 of them can be (in fact, should be) expressed in terms of the remaining 20. The conditions (9) and (10) are *positivity* conditions which ensure that the artificial contributions to the energy of the system due to the discontinuous nature of the approximation are non-negative. The condition (11) is a mild restriction on the geometry of the arch, namely, it ensures that the arch is either locally not *too curved*, or equivalently the mesh is fine enough.

3. Post-processing

Next, we describe the post-processing

$$\boldsymbol{\varphi}_h^* := (T_h^*, N_h^*, M_h^*, \theta_h^*, u_h^*, w_h^*)$$

of the approximate solution $\boldsymbol{\varphi}_h = (T_h, N_h, M_h, \theta_h, u_h, w_h)$ provided by the DG method. It is based on the fact that the numerical traces superconverge at each of the nodes with order $2k+1$. To state this result we need to introduce some notation. We define the error of approximation as

$$e_\varphi = \varphi - \varphi_h, \qquad \widehat{e}_\varphi = \varphi - \widehat{\varphi}_h,$$

for any $\varphi \in \{T, N, M, \theta, u, w\}$, and set

$$\boldsymbol{e} = \boldsymbol{\varphi} - \boldsymbol{\varphi}_h, \qquad \widehat{\boldsymbol{e}} = \boldsymbol{\varphi} - \widehat{\boldsymbol{\varphi}}_h.$$

Here

$$\boldsymbol{\varphi} := (T, N, M, \theta, u, w)$$

denotes the exact solution of the governing equations (2). The error in the numerical traces of φ_h is defined as

$$\|\widehat{e}_\varphi\|_\infty := \|\widehat{e}_\varphi\|_{\ell^\infty(\mathcal{E}_h)} := \max_{x_j \in \mathcal{E}_h} |\widehat{e}_\varphi(x_j)|,$$

and the global error in the numerical traces is set to be

$$\|\widehat{\boldsymbol{e}}\|_\infty := \max_{\varphi \in \{T,N,M,\theta,u,w\}} \|\widehat{e}_\varphi\|_\infty.$$

We denote by $\|\cdot\|_{s,D}$ and $|\cdot|_{s,D}$ the usual norm and seminorm, respectively, in the Sobolev space $H^s(D)$ where D is any subset of Ω_h. We drop the subindex D whenever $D = \Omega_h$ or $D = \Omega$. We set, for $\boldsymbol{u} = (u_1, u_2, u_3, u_4, u_5, u_6)$,

$$|\boldsymbol{u}|_{s,D} := (|u_1|_{s,D}^2 + |u_2|_{s,D}^2 + |u_3|_{s,D}^2 + |u_4|_{s,D}^2 + |u_5|_{s,D}^2 + |u_6|_{s,D}^2)^{1/2}.$$

In [5] the following wide family of DG methods has been analyzed. They are defined by setting the functions C_{ij} as follows.

$$C_{16} = C_{25} = C_{34} = C_{43} = C_{52} = C_{61} = -\mathsf{c} \tag{12}$$

for all x in $\mathcal{E}_h$, except

$$C_{16} = C_{25} = C_{34} = 0 \quad \text{on} \quad \partial\Omega. \tag{13}$$

Here, $\mathsf{c} > 0$ is any constant which is independent of the mesh size h. We assume that

$$C_{ij}^2 \le \mathsf{c} \quad \text{ for all } i, j = 1, \dots, 6, \tag{14}$$

and that

$$(C_{ii}(x) - 1/2)^2 \le \mathsf{c} \quad \text{ for all } i = 1, \dots, 6. \tag{15}$$

Such a choice can be obtained, for example, by setting

$$C_{16} = C_{25} = C_{34} = C_{43} = C_{52} = C_{61} = -1$$

for all x in $\mathcal{E}_h$, except

$$C_{16} = C_{25} = C_{34} = 0 \quad \text{on} \quad \partial\Omega,$$

and setting all the remaining C_{ij}'s to zero.

We are now ready to state the superconvergence result for the numerical traces.

Theorem 3.1. ([5]) *Let $k \geq 0$ be a polynomial degree and suppose that $\boldsymbol{\varphi}$ belongs to $[H^{k+1}(\Omega_h)]^6$. Let $\boldsymbol{\varphi}_h$ be the DG solution defined by the weak formulation* (4), *and the numerical traces* (5)–(7) *where the functions C_{ij} are defined so as to satisfy* (12)–(15). *Then,*

$$\|\boldsymbol{\varphi} - \widehat{\boldsymbol{\varphi}}_h\|_\infty \leq C\, h^{2k+1} |\boldsymbol{\varphi}|_{k+1} \tag{16}$$

for some constant C independent of h and d.

Our post-processing is defined in an element-by-element fashion as follows. On the element $I_j = (x_{j-1}, x_j)$, $1 \leq j \leq \mathcal{N}$, we define the post-processed solution

$$\boldsymbol{\varphi}_h^* = (T_h^*, N_h^*, M_h^*, \theta_h^*, u_h^*, w_h^*)$$

as the element of the space $[P^{2k}(I_j)]^6$ in four simple steps as follows.
Step 1: Compute T_h^* and N_h^* by solving

$$-(T_h^*, v_1')_{I_j} + T_h^*(x_j^-)v_1(x_j^-) + (\kappa N_h^*, v_1)_{I_j} = (q, v_1)_{I_j} + \widehat{T}_h(x_{j-1})v_1(x_{j-1}^+), \tag{17a}$$

$$-(N_h^*, v_2')_{I_j} + N_h^*(x_j^-)v_2(x_j^-) - (\kappa T_h^*, v_2)_{I_j} = (p, v_2)_{I_j} + \widehat{N}_h(x_{j-1})v_2(x_{j-1}^+), \tag{17b}$$

for all v_1 and v_2 in $P^{2k}(I_j)$.
Step 2: Compute M_h^* by solving

$$-(M_h^*, v_3')_{I_j} + M_h^*(x_j^-)v_3(x_j^-) = (T_h^*, v_3)_{I_j} + \widehat{M}_h(x_{j-1})v_3(x_{j-1}^+), \tag{18}$$

for all v_3 in $P^{2k}(I_j)$.
Step 3: Compute θ_h^* by solving

$$-(\theta_h^*, v_4')_{I_j} + \theta_h^*(x_j^-)v_4(x_j^-) = (M_h^*, v_4)_{I_j} + \widehat{\theta}_h(x_{j-1})v_4(x_{j-1}^+), \tag{19}$$

for all v_4 in $P^{2k}(I_j)$.
Step 4: Compute u_h^* and w_h^* by solving

$$\begin{aligned} -(u_h^*, v_5')_{I_j} + u_h^*(x_j^-)v_5(x_j^-) - (\kappa w_h^*, v_5)_{I_j} & \\ = d^2(N_h^*, v_5)_{I_j} + \widehat{u}_h(x_{j-1})v_5(x_{j-1}^+), & \end{aligned} \tag{20a}$$

$$\begin{aligned} -(w_h^*, v_6')_{I_j} + w_h^*(x_j^-)v_6(x_j^-) + (\kappa u_h^*, v_6)_{I_j} & \\ = d^2(T_h^*, v_6)_{I_j} - (\theta_h^*, v_6)_{I_j} + \widehat{w}_h(x_{j-1})v_6(x_{j-1}^+), & \end{aligned} \tag{20b}$$

for all v_5 and v_6 in $P^{2k}(I_j)$.

Next, we state a theorem about the existence and uniqueness of the post-processed solution.

Theorem 3.2. *Consider the post-processing defined by* (17)–(20) *on an arbitrary element $I_j \in \Omega_h$. These equations define a unique solution $\boldsymbol{\varphi}_h^* = (T_h^*, N_h^*, M_h^*, \theta_h^*, u_h^*, w_h^*)$ provided that the condition* (11) *is satisfied whenever κ is not identically equal to a constant on I_j.*

Remark 3.3. If κ is identically constant, i.e. the arch is locally circular or flat, on an element I_j then the condition (11) is not necessary, and the post-processing automatically defines a unique solution.

It is not difficult to see that the equations (17)–(20) are the discretization by the classical DG method [14, 13] of the following system of initial value problems

$$(T^*)' + \kappa N^* = q \quad \text{in } I_j, \quad T^*(x_{j-1}) = \widehat{T}_h(x_{j-1}), \tag{21a}$$

$$(N^*)' - \kappa T^* = p \quad \text{in } I_j, \quad N^*(x_{j-1}) = \widehat{N}_h(x_{j-1}), \tag{21b}$$

$$(M^*)' = T^* \quad \text{in } I_j, \quad M^*(x_{j-1}) = \widehat{M}_h(x_{j-1}), \tag{21c}$$

$$(\theta^*)' = M^* \quad \text{in } I_j, \quad \theta^*(x_{j-1}) = \widehat{\theta}_h(x_{j-1}), \tag{21d}$$

$$(u^*)' - \kappa w^* = d^2 N^* \quad \text{in } I_j, \quad u^*(x_{j-1}) = \widehat{u}_h(x_{j-1}), \tag{21e}$$

$$(w^*)' + \kappa u^* = d^2 T^* - \theta^* \quad \text{in } I_j, \quad w^*(x_{j-1}) = \widehat{w}_h(x_{j-1}). \tag{21f}$$

Its step-by-step nature reveals that when defining the post-processing (17)–(20) we made use of the fact that the system of equations (21) is partially decoupled in the following sense. It is possible to solve for T^* and N^* using only the equations (21a) and (21b). Then we can insert T^* into (21c) and solve for M^*, and then insert M^* into (21d) to solve for θ^*. Finally, we may insert N^* into (21e), and T^* and θ^* into (21f), and solve for u^* and w^*.

Based on the above observation, we can rewrite (21) in a single framework as follows:

$$(\boldsymbol{\varphi}_\ell^*)' - A_\ell \boldsymbol{\varphi}_\ell^* = \boldsymbol{f}_\ell^* \quad \text{in } I_j, \qquad \boldsymbol{\varphi}_\ell^*(x_{j-1}) = \widehat{\boldsymbol{\varphi}}_\ell(x_{j-1}) \tag{22}$$

for $\ell = 1, 2, 3, 4$. Here,

$$\boldsymbol{\varphi}_1^* := \begin{bmatrix} T^* \\ N^* \end{bmatrix}, \qquad \boldsymbol{\varphi}_2^* := [\, M^*], \quad \boldsymbol{\varphi}_3^* := [\, \theta^*], \quad \boldsymbol{\varphi}_4^* := \begin{bmatrix} u^* \\ w^* \end{bmatrix},$$

and similarly for $\widehat{\boldsymbol{\varphi}}_\ell^*$,

$$A_1 := \begin{bmatrix} 0 & -\kappa \\ \kappa & 0 \end{bmatrix}, \quad A_2 = [0], \qquad A_3 = [0], \qquad A_4 = \begin{bmatrix} 0 & \kappa \\ -\kappa & 0 \end{bmatrix},$$

$$\boldsymbol{f}_1^* = \begin{bmatrix} q \\ p \end{bmatrix}, \qquad \boldsymbol{f}_2^* := [T^*], \quad \boldsymbol{f}_3^* := [M^*], \quad \boldsymbol{f}_4^* := \begin{bmatrix} d^2 N^* \\ d^2 T^* - \theta^* \end{bmatrix}.$$

Consequently, we can reformulate the post-processing defined by the equations (17)–(20) in the following unified framework. Find $(\boldsymbol{\varphi}_{1,h}^*, \boldsymbol{\varphi}_{2,h}^*, \boldsymbol{\varphi}_{3,h}^*, \boldsymbol{\varphi}_{4,h}^*,) \in [P^{2k}(I_j)]^2 \times P^{2k}(I_j) \times P^{2k}(I_j) \times [P^{2k}(I_j)]^2$ such that

$$\begin{aligned} -(\boldsymbol{\varphi}_{\ell,h}^*, \boldsymbol{v}_\ell')_{I_j} + \boldsymbol{\varphi}_{\ell,h}^*(x_j^-) \cdot \boldsymbol{v}_\ell(x_j^-) - (A_\ell \boldsymbol{\varphi}_{\ell,h}^*, \boldsymbol{v}_\ell)_{I_j} \\ = (\boldsymbol{f}_\ell^*, \boldsymbol{v}_\ell)_{I_j} + \widehat{\boldsymbol{\varphi}}_{\ell,h}(x_{j-1}) \cdot \boldsymbol{v}_\ell(x_{j-1}^+) \end{aligned} \tag{23}$$

for all $(\boldsymbol{v}_1, \boldsymbol{v}_2, \boldsymbol{v}_3, \boldsymbol{v}_4) \in [P^{2k}(I_j)]^2 \times P^{2k}(I_j) \times P^{2k}(I_j) \times [P^{2k}(I_j)]^2$. Here we have used the obvious definitions of $\boldsymbol{\varphi}_{\ell,h}^*$ and $\widehat{\boldsymbol{\varphi}}_{\ell,h}$, and A_ℓ and $\boldsymbol{f}_\ell^*$ are the same as above. We have also employed the following notation. For two vector-valued functions $\boldsymbol{\varphi}$ and $\boldsymbol{v}$ in $[L^2(I_j)]^m$

$$(\boldsymbol{\varphi}, \boldsymbol{v})_{I_j} := \int_{I_j} \boldsymbol{\varphi} \cdot \boldsymbol{v} = \sum_{i=1}^m \int_{I_j} \varphi_i v_i,$$

and " $\cdot$ " denotes the usual dot product of two vectors in $\mathbb{R}^m$.

Next, we state our main result.

Theorem 3.4. *Under the hypotheses of Theorem 3.1, the error of the post-processed approximation is such that*

$$\|\boldsymbol{\varphi} - \boldsymbol{\varphi}_h^*\|_{0,\Omega_h} \leq C\, h^{2k+1} \tag{24}$$

for some constant C independent of h and d.

Remark 3.5. This theorem extends earlier results by Celiker and Cockburn for DG methods for convection-diffusion problems in [3], and for Timoshenko beams in [2]. The main difficulty here arises from considering an arbitrary geometry for the arch which results in the appearance of the additional variables u and N in the governing equations. Moreover, the transverse displacement u is coupled with the tangential displacement w, and the shear stress T is coupled with the membrane stress N, as can be seen from (2a)–(2b) and (2e)–(2f), respectively. Consequently, for the post-processing we have to solve a system of equations, rather than a set of scalar equations, as is evident from (22). This renders the analysis of the post-processing of DG methods for arches considerably more involved than that of the DG methods for beams. Let us note that extending a result for beams to one for arches is analogous to extending a result for plates to one for shells and hence poses several challenges.

Remark 3.6. Since the constant C appearing in the estimate (24) is independent of the thickness parameter d, the post-processed solution is free from shear and membrane locking.

Remark 3.7. The estimate (24) shows that the post-processed approximation converges with order $2k+1$ throughout the computational domain. This should be contrasted with the fact that before post-processing the approximation converges with the optimal order or $k+1$. Hence, for $k \geq 1$, the order of convergence is almost doubled by the local post-processing.

Remark 3.8. The value of the increase in the convergence order mentioned in the above remark becomes more evident if we calculate the computational cost of this post-processing. Since it is performed in an element-by-element fashion the total cost is $\mathcal{N}$ times the cost on one element. Therefore it is extremely inexpensive. More explicitly, Steps 1 and 4 require solving linear systems of order $2(2k+1)$, and Steps 2 and 3 can be performed by inverting a single linear system of order $2k+1$. It is thus easy to see that the computational cost of the post-processing is negligible when compared to that of computing the original DG solution which, in general, requires solving a linear system of order $6\mathcal{N}(k+1)$.

4. Proofs

In this section we give detailed proofs of our results in Section 3. We begin with the proof of Theorem 3.2. It is based on the following lemma which was proved in [5]. We also provide a proof here for the sake of completeness.

Lemma 4.1. *Let r be a non-negative integer. Let $f, g \in P^r([a,b])$ be such that*

$$f(a) = g(a) = 0. \tag{25}$$

Suppose that

$$\mathsf{P}_r(g' + \alpha f) = 0 \quad \text{and} \quad \mathsf{P}_r(f' - \alpha g) = 0, \tag{26}$$

where α is a function in $L^\infty([a,b])$ and P_r denotes the L^2-orthogonal projection into $P^r([a,b])$. Then $f = g = 0$ in $[a,b]$ if

[(a)]α is identically equal to a constant, or α is not identically equal to a constant and

$$b - a \leq \frac{1}{2\|\alpha - \overline{\alpha}\|_{L^\infty([a,b])}} \tag{27}$$

where $\overline{\alpha}$ denotes the average value of α over the interval $[a,b]$.

(2) *Proof.* By (26), we have that

$$g' + \mathsf{P}_r(\alpha f) = 0, \tag{28a}$$

$$f' - \mathsf{P}_r(\alpha g) = 0, \tag{28b}$$

pointwise on $[a, b]$. Multiplying (28a) by g and (28b) with f we get

$$\frac{1}{2}(g^2)' + g\mathsf{P}_r(\alpha f) = 0, \qquad \frac{1}{2}(f^2)' - f\mathsf{P}_r(\alpha g) = 0,$$

and hence

$$\frac{1}{2}(g^2 + f^2)' = f\mathsf{P}_r(\alpha g) - g\mathsf{P}_r(\alpha f) = f\mathsf{P}_r((\alpha - \overline{\alpha})g) - g\mathsf{P}_r((\alpha - \overline{\alpha})f) \tag{29}$$

since $-f\mathsf{P}_r(\overline{\alpha}g) + g\mathsf{P}_r(\overline{\alpha}f) = 0$ because $\overline{\alpha}$ is a constant and $f, g \in P^r([a, b])$. Integrating both sides of (29) from a to an arbitrary x in $[a, b]$, and using (25), we obtain

$$\frac{1}{2}(g^2 + f^2)(x) = T_1(x) + T_2(x)$$

where

$$T_1(x) = \int_a^x f(s)\mathsf{P}_r((\alpha - \overline{\alpha})g)(s)\, ds, \qquad T_2(x) = -\int_a^x g(s)\mathsf{P}_r((\alpha - \overline{\alpha})f)(s)\, ds.$$

By Cauchy-Schwarz inequality

$$\begin{aligned} |T_1(x)| &\le \|f\|_{L^2([a,b])}\|(\alpha - \overline{\alpha})g\|_{L^2([a,b])} \\ &\le \|\alpha - \overline{\alpha}\|_{L^\infty([a,b])}\|f\|_{L^2([a,b])}\|g\|_{L^2([a,b])}. \end{aligned}$$

Similarly,

$$|T_2(x)| \le \|\alpha - \overline{\alpha}\|_{L^\infty([a,b])}\|f\|_{L^2([a,b])}\|g\|_{L^2([a,b])},$$

and hence

$$\frac{1}{2}(g^2 + f^2)(x) \le 2\|\alpha - \overline{\alpha}\|_{L^\infty([a,b])}\|f\|_{L^2([a,b])}\|g\|_{L^2([a,b])}.$$

Integrating both sides over $x \in [a, b]$ implies

$$\begin{aligned} \frac{1}{2}(\|f\|^2_{L^2([a,b])} + \|g\|^2_{L^2([a,b])}) &\le 2(b-a)\|\alpha - \overline{\alpha}\|_{L^\infty([a,b])}\|f\|_{L^2([a,b])}\|g\|_{L^2([a,b])} \\ &\le (b-a)\|\alpha - \overline{\alpha}\|_{L^\infty([a,b])}(\|f\|^2_{L^2([a,b])} + \|g\|^2_{L^2([a,b])}) \end{aligned}$$

by Young's inequality. Thus,

$$\left[\frac{1}{2} - (b-a)\|\alpha - \overline{\alpha}\|_{L^\infty([a,b])}\right](\|f\|^2_{L^2([a,b])} + \|g\|^2_{L^2([a,b])}) \le 0. \tag{30}$$

Now, if α is identically constant on $[a, b]$ then $\overline{\alpha} = \alpha$ and the result follows since in such a case (30) implies $\|f\|^2_{L^2([a,b])} + \|g\|^2_{L^2([a,b])} = 0$. If α is not identically constant on $[a, b]$ then we reach the same conclusion by (27).

This completes the proof. ∎

We are now ready to prove Theorem 3.2.

Proof. (Theorem 3.2) We only prove the existence and uniqueness of Step 1 of the post-processing. Steps 2 and 3 are well defined since they are nothing but the classical DG method applied to first order problems on a single element. Step 4 is almost identical to Step 1.

Due to the linearity of the problem it suffices to show that the only solution to (17) with

$$p = q = 0 \quad \text{in } I_j,$$

and

$$\widehat{T}_h(x_{j-1}) = \widehat{N}_h(x_{j-1}) = 0,$$

is

$$T_h^* = N_h^* = 0 \quad \text{in } I_j.$$

In this case, the equations (17) simplify to

$$-(T_h^*, v_1')_{I_j} + T_h^*(x_j^-)v_1(x_j^-) + (\kappa N_h^*, v_1)_{I_j} = 0, \tag{31a}$$

$$-(N_h^*, v_2')_{I_j} + N_h^*(x_j^-)v_2(x_j^-) - (\kappa T_h^*, v_2)_{I_j} = 0, \tag{31b}$$

Taking $v_1 = T_h^*$ in (31a) and $v_2 = N_h^*$ in (31b), and adding the resulting equations we get

$$-(T_h^*, (T_h^*)')_{I_j} + (T_h^*(x_j^-))^2 - (N_h^*, (N_h^*)')_{I_j} + (N_h^*(x_j^-))^2 = 0.$$

This implies,

$$\frac{1}{2}\left[(T_h^*)^2(x_{j-1}^+) + (T_h^*)^2(x_j^-)\right] + \frac{1}{2}\left[(N_h^*)^2(x_{j-1}^+) + (N_h^*)^2(x_j^-)\right] = 0.$$

Hence,

$$T_h^*(x_{j-1}^+) = T_h^*(x_j^-) = N_h^*(x_{j-1}^+) = N_h^*(x_j^-) = 0. \tag{32}$$

This further simplifies (31) to

$$\begin{aligned} -(T_h^*, v_1')_{I_j} + (\kappa N_h^*, v_1)_{I_j} &= 0, \\ -(N_h^*, v_2')_{I_j} - (\kappa T_h^*, v_2)_{I_j} &= 0, \end{aligned}$$

Upon a simple integration by parts and invoking (32) we get that

$$((T_h^*)' + \kappa N_h^*, v_1)_{I_j} = 0, \quad \text{and} \quad ((N_h^*)' - \kappa T_h^*, v_2)_{I_j} = 0.$$

for all v_1 and v_2 in $P^r([a,b])$. In other words,

$$\mathsf{P}_r((T_h^*)' + \kappa N_h^*, v_1) = 0, \quad \text{and} \quad \mathsf{P}_r((N_h^*)' - \kappa T_h^*, v_2) = 0.$$

The result now follows from Lemma 4.1. $\square$

Next, we prove Theorem 3.4. Recall that we were able to put our post-processing into a single framework given by (23) as an approximation to the first-order system of ODEs (22). This motivates the study of the following more general initial value problem

$$\begin{aligned} \boldsymbol{u}'(x) - A(x)\boldsymbol{u}(x) &= \boldsymbol{f}(x) \quad \text{for } x \in K = (a,b), \\ \boldsymbol{u}(a) &= \boldsymbol{u}_a \end{aligned} \tag{33}$$

where $\boldsymbol{u} : [a,b] \to \mathbb{R}^m$, for some integer $m \geq 1$, is the unknown function, and $\boldsymbol{f} : [a,b] \to \mathbb{R}^m$ is a given function. We assume that A is a given $m \times m$ matrix such that there exists a unique solution to (33). Observe that such a condition is satisfied for the cases we are interested in this paper.

Let $r \geq 0$ be a polynomial degree and suppose that we approximate $\boldsymbol{u}$ by the function $\boldsymbol{u}_h \in [P^r(K)]^m$ defined by requiring that the equation

$$-(\boldsymbol{u}_h, \boldsymbol{v}')_K + \boldsymbol{u}_h(b^-) \cdot \boldsymbol{v}(b^-) - (A\boldsymbol{u}_h, \boldsymbol{v})_K = (\boldsymbol{f}^*, \boldsymbol{v})_K + \boldsymbol{u}_a^* \cdot \boldsymbol{v}(a^+) \tag{34}$$

holds for all $\boldsymbol{v} \in [P^r(K)]^m$. Here, $\boldsymbol{f}^*$ is an approximation to $\boldsymbol{f}$ such that

$$\|\boldsymbol{f} - \boldsymbol{f}^*\|_{0,K} \leq C\, h_K^{r+1}, \tag{35}$$

and $\boldsymbol{u}_a^*$ is an approximation to $\boldsymbol{u}_a$ such that

$$|\boldsymbol{u}_a - \boldsymbol{u}_a^*| \leq C\, h_K^{r+1} \tag{36}$$

where $h_K = b - a$. The magnitude of the vector $\boldsymbol{v} \in \mathbb{R}^m$ is denoted by $|\boldsymbol{v}|$, and we have extended the definitions of Sobolev norms and seminorms to vector-valued functions in an obvious fashion. We assume that the matrix A is such that the method (34) defines a unique solution. We also suppose that all the components of the matrix A, and of the vector-valued functions $\boldsymbol{f}$ and $\boldsymbol{f}^*$ are in $H^{r+1}(K)$.

It is not difficult to see that the proof of Theorem 3.4 follows from a successive application of the following theorem which provides an optimal error estimate for the method defined by (34).

Theorem 4.2. *Suppose that we approximate the solution of the initial value problem* (33) *by the method* (34). *Then, for sufficiently small h_K, we have the error estimate*

$$\|\boldsymbol{u} - \boldsymbol{u}_h\|_{0,K} \leq C h_K^{r+1} \tag{37}$$

where C is a constant independent of h_K.

Remark 4.3. More general DG methods were introduced and analyzed for the initial value problem (33) by Delfour *et al.* in [9]. They have proved optimal error estimates as in (37). The same problem has also been studied by Erikkson *et al.* in [11], and by Thomée in [17]. They have proved optimal L^∞ error estimates under more restrictive regularity requirements. Moreover, their analysis is restricted to symmetric and positive definite A.

Remark 4.4. Observe that the method (34) differs from those studied in [9, 11, 17] in the sense that we have to use *approximate data* $\boldsymbol{f}^*$ and $\boldsymbol{u}_a^*$ since this is precisely what we need for our purposes. Moreover, the analysis we provide in this paper is significantly different from the ones that have appeared in the literature. More explicitly, we employ projection operators tailored to the special structure of the method.

Next we describe these projection operators. For any $\psi \in H^1(K)$, the function $\pi^{\pm}\psi \in P^r(K)$ is defined on the interval $K = [a, b]$ by

$$(\psi - \pi^{\pm}\psi, v)_K = 0 \qquad \forall v \in P^{r-1}(K), \quad \text{if } r > 0, \tag{38a}$$

$$(\pi^{-}\psi)(b^{-}) = \psi(b^{-}), \qquad (\pi^{+}\psi)(a^{+}) = \psi(a^{+}). \tag{38b}$$

The projection operators $\boldsymbol{\pi}^{\pm}$ acting on vector-valued functions $\boldsymbol{\psi} : K \to \mathbb{R}^m$ are defined by (38) applied to each component function. Notwithstanding the fact that these projection operators have been widely used for the analysis of DG methods applied to various problems, [1, 2, 3, 6, 8, 10, 12, 15, 18] in our analysis we uncover a new superconvergence property of the projection of the error which, to the best of our knowledge, has not appeared in the literature for the analysis of DG methods for the initial value problem (33).

The approximation properties of $\boldsymbol{\pi}^{\pm}$, namely, that there exists a constant C independent of $\boldsymbol{\psi}$ such that

$$\|\boldsymbol{\psi} - \boldsymbol{\pi}^{\pm}\boldsymbol{\psi}\|_{0,K} \leq C h_k^{s+1} |\boldsymbol{\psi}|_{s+1,K} \tag{39}$$

for any $s \in [0, r]$, can be found in the references cited above. Theorem 4.2 follows from the above approximation property, the triangle inequality

$$\|\boldsymbol{u} - \boldsymbol{u}_h\|_{0,K} \leq \|\boldsymbol{u} - \boldsymbol{\pi}^{-}\boldsymbol{u}\|_{0,K} + \|\boldsymbol{\pi}^{-}\boldsymbol{u} - \boldsymbol{u}_h\|_{0,K},$$

and the following superconvergence result for $\boldsymbol{\pi}^{-}\boldsymbol{e}_{\boldsymbol{u}}$.

Theorem 4.5. *Suppose that h_K is sufficiently small. Then, we have that*

$$\|\boldsymbol{\pi}^{-}\boldsymbol{e_u}\|_{0,K} \leq C\, h_K^{r+3/2} \tag{40}$$

where C is a constant which is independent of h_K. Moreover, if

$$|\boldsymbol{u}_a - \boldsymbol{u}_a^*| \leq C h_K^{r+3/2}, \qquad \text{or} \qquad \boldsymbol{u}_a = \boldsymbol{u}_a^*, \tag{41}$$

then

$$\|\boldsymbol{\pi}^{-}\boldsymbol{e_u}\|_{0,K} \leq C\, h_K^{r+2}. \tag{42}$$

The proof of this theorem will be based on a duality argument. We thus begin with introducing the dual problem for any given $\boldsymbol{\eta} : K = [a,b] \to \mathbb{R}^m$ in $L^2(K)$:

$$\boldsymbol{\psi}' + A^T\boldsymbol{\psi} = \boldsymbol{\eta} \quad \text{in } K, \tag{43a}$$

$$\boldsymbol{\psi}(b) = \mathbf{0}. \tag{43b}$$

We have the following regularity for the solution of this problem.

Lemma 4.6. *Let $\boldsymbol{\psi}$ be the solution of* (43)*. Then*

$$|\boldsymbol{\psi}|_{1,K} + \frac{1}{h_K}\|\boldsymbol{\psi}\|_{0,K} \;\leq\; C\|\boldsymbol{\eta}\|_{0,K}, \tag{44}$$

where the constant C is independent of the datum $\boldsymbol{\eta}$.

Proof. By the basic theory of first order linear systems of differential equations we have, for any $\sigma \in [a,b]$, that

$$\boldsymbol{\psi}(x) = \boldsymbol{\Psi}(x)\boldsymbol{\Psi}^{-1}(\sigma)\,\boldsymbol{\psi}(\sigma) + \boldsymbol{\Psi}(x)\int_\sigma^x \boldsymbol{\Psi}^{-1}(s)\boldsymbol{\eta}(s)\,ds$$

where $\boldsymbol{\Psi}(\cdot)$ is the fundamental matrix associated with $-A^T$. Thus, due to the zero boundary condition at $x = b$, (43b),

$$\boldsymbol{\psi}(x) = \boldsymbol{\Psi}(x)\int_b^x \boldsymbol{\Psi}^{-1}(s)\boldsymbol{\eta}(s)\,ds.$$

The boundedness of $\boldsymbol{\Psi}$ and $\boldsymbol{\Psi}'$ imply

$$|\boldsymbol{\psi}|_{1,K} \leq C|\boldsymbol{g}|_{1,K} \quad \text{and} \quad \|\boldsymbol{\psi}\|_{0,K} \leq C\|\boldsymbol{g}\|_{0,K}$$

where $\boldsymbol{g} := \int_b^x \boldsymbol{\eta}(s)\,ds$. The first part of the regularity estimate (44) then follows from the fact that $|\boldsymbol{g}|_{1,K} = \|\boldsymbol{g}'\|_{0,K} = \|\boldsymbol{\eta}\|_{0,K}$. To prove the second part, we get, by a simple application of Cauchy-Schwarz inequality that

$$\begin{aligned}
\|\boldsymbol{\psi}\|_{0,K}^2 \leq C\|\boldsymbol{g}\|_{0,K}^2 &= C\int_a^b \left[\int_b^x \boldsymbol{\eta}(s)ds\right]^2 dx \\
&\leq C\int_a^b \Big|\int_b^x ds\Big|\Big|\int_b^x |\boldsymbol{\eta}(s)|^2 ds\Big|\, dx \\
&\leq C\, h_K\|\boldsymbol{\eta}\|_{0,K}^2 \int_a^b dx \\
&= C\, h_K^2\|\boldsymbol{\eta}\|_{0,K}^2.
\end{aligned}$$

Hence, $\|\boldsymbol{\psi}\|_{0,K} \leq C\, h_K\|\boldsymbol{\eta}\|_{0,K}$. This finishes the proof. □

As expected, one of the main ingredients of our error analysis is an error equation. Inserting the exact solution $\boldsymbol{u}$ of (33) into the DG formulation (34) we get

$$-(e_{\boldsymbol{u}}, \boldsymbol{v}')_K + e_{\boldsymbol{u}}(b^-)\cdot\boldsymbol{v}(b^-) - (Ae_{\boldsymbol{u}}, \boldsymbol{v})_K = (\boldsymbol{f} - \boldsymbol{f}^*, \boldsymbol{v})_K + (\boldsymbol{u}_a - \boldsymbol{u}_a^*)\cdot\boldsymbol{v}(a^+) \tag{45}$$

for all $\boldsymbol{v} \in [P^r(K)]^m$. Note that the quantity on the right-hand side can be viewed as a *consistency error* due to the fact that we are approximating the solution $\boldsymbol{u}$ of (33) by using *approximate* data $\boldsymbol{f}^*$ and $\boldsymbol{u}_a^*$. If the data are exact, namely, $\boldsymbol{f} = \boldsymbol{f}^*$ and $\boldsymbol{u}_a^* = \boldsymbol{u}_a$ then we recover a classical Galerkin orthogonality property.

The orthogonality property (38a) of the projection operator $\boldsymbol{\pi}^-$, and some simple algebraic manipulations yield an alternative form of (45) which is more amenable to our analysis

$$\begin{aligned} -(\boldsymbol{\pi}^- e_{\boldsymbol{u}}, \boldsymbol{v}')_K + (\boldsymbol{\pi}^- e_{\boldsymbol{u}})(b^-) \cdot \boldsymbol{v}(b^-) - (A\,\boldsymbol{\xi}_{\boldsymbol{u}}^-, \boldsymbol{v})_K - (A\,\boldsymbol{\pi}^- e_{\boldsymbol{u}}, \boldsymbol{v})_K \\ = (\boldsymbol{f} - \boldsymbol{f}^*, \boldsymbol{v})_K + (\boldsymbol{u}_a - \boldsymbol{u}_a^*) \cdot \boldsymbol{v}(a^+) \end{aligned} \tag{46}$$

where we have introduced the notation

$$\boldsymbol{\xi}_{\boldsymbol{u}}^{\pm} := \boldsymbol{u} - \boldsymbol{\pi}^{\pm}\boldsymbol{u}. \tag{47}$$

Next, we state a technical lemma.

Lemma 4.7. *Consider the dual problem* (43) *and the method* (34) *approximating the solution of* (33). *Then we have the following representation formula*

$$\begin{aligned} (\boldsymbol{\pi}^- e_{\boldsymbol{u}}, \boldsymbol{\eta})_K = &- (A\,\boldsymbol{\xi}_{\boldsymbol{u}}^-, \boldsymbol{\psi})_K &&+ (A\,\boldsymbol{\xi}_{\boldsymbol{u}}^-, \boldsymbol{\xi}_{\boldsymbol{\psi}}^+)_K + (A\,\boldsymbol{\pi}^- e_{\boldsymbol{u}}, \boldsymbol{\xi}_{\boldsymbol{\psi}}^+)_K \\ &- (\boldsymbol{f} - \boldsymbol{f}^*, \boldsymbol{\pi}^+\boldsymbol{\psi})_K &&- (\boldsymbol{u}_a - \boldsymbol{u}_a^*) \cdot (\boldsymbol{\pi}^+\boldsymbol{\psi})(a^+). \end{aligned} \tag{48}$$

We delay the proof of this lemma to the end of this section.

We are now ready to prove Theorem 4.5.

Proof. (Theorem 4.5) Setting $\boldsymbol{\eta} = \boldsymbol{\pi}^- e_{\boldsymbol{u}}$ in (48) gives

$$\|\boldsymbol{\pi}^- e_{\boldsymbol{u}}\|_{0,K}^2 = \sum_{i=1}^{5} T_i \tag{49}$$

where

$$\begin{aligned} T_1 &= -(A\boldsymbol{\xi}_{\boldsymbol{u}}^-, \boldsymbol{\psi})_K, \\ T_2 &= (A\,\boldsymbol{\xi}_{\boldsymbol{u}}^-, \boldsymbol{\xi}_{\boldsymbol{\psi}}^+)_K, \\ T_3 &= (A\,\boldsymbol{\pi}^- e_{\boldsymbol{u}}, \boldsymbol{\xi}_{\boldsymbol{\psi}}^+)_K, \\ T_4 &= -(\boldsymbol{f} - \boldsymbol{f}^*, \boldsymbol{\pi}^+\boldsymbol{\psi})_K, \\ T_5 &= -(\boldsymbol{u}_a - \boldsymbol{u}_a^*) \cdot (\boldsymbol{\pi}^+\boldsymbol{\psi})(a^+). \end{aligned}$$

An estimate of $\|\boldsymbol{\pi}^- e_{\boldsymbol{u}}\|_{0,K}$ now follows by estimating T_i for $i = 1, \dots, 5$. By Cauchy-Schwarz inequality we have

$$|T_1| \ \le\ \|A\boldsymbol{\xi}_{\boldsymbol{u}}^-\|_{0,K}\|\boldsymbol{\psi}\|_{0,K} \ \le\ C\|\boldsymbol{\xi}_{\boldsymbol{u}}^-\|_{0,K}\|\boldsymbol{\psi}\|_{0,K}$$

where we have used the regularity assumption on the matrix A, namely, that all component of A are in $H^{r+1}(K)$, and hence in $L^2(K)$. By the approximation properties, (39), of $\boldsymbol{\pi}^-$, and the regularity of the dual problem, (44), we have that

$$\begin{aligned} |T_1| &\le C\,h_K^{r+1}|\boldsymbol{u}|_{r+1,K} \ \cdot\ Ch_K\|\boldsymbol{\eta}\|_{0,K} \\ &\le C\,h_K^{r+2}\|\boldsymbol{\pi}^- e_{\boldsymbol{u}}\|_{0,K} \end{aligned} \tag{50}$$

where we have absorbed $|\boldsymbol{u}|_{r+1,K}$ in the constant C. Similarly,

$$\begin{aligned} |T_2| &\le \|A\boldsymbol{\xi}_{\boldsymbol{u}}^-\|_{0,K}\|\boldsymbol{\xi}_{\boldsymbol{\psi}}^+\|_{0,K} \\ &\le C\,h_K^{r+1}|\boldsymbol{u}|_{r+1,K} \ \cdot\ C\,h_K|\boldsymbol{\psi}|_{1,K} \\ &\le C\,h_K^{r+2}|\boldsymbol{u}|_{r+1,K}|\boldsymbol{\psi}|_{1,K} \\ &\le C\,h_K^{r+2}\|\boldsymbol{\pi}^- e_{\boldsymbol{u}}\|_{0,K}, \end{aligned} \tag{51}$$

and

$$
\begin{aligned}
|T_3| &\le \|A\boldsymbol{\pi}^- e_{\boldsymbol{u}}\|_{0,K}\|\boldsymbol{\xi}^+_{\boldsymbol{\psi}}\|_{0,K} \\
&\le C\|\boldsymbol{\pi}^- e_{\boldsymbol{u}}\|_{0,K} \;\cdot\; C\,h_K|\boldsymbol{\psi}|_{1,K} \\
&\le C\,h_K\|\boldsymbol{\pi}^- e_{\boldsymbol{u}}\|_{0,K}|\boldsymbol{\psi}|_{1,K} \\
&\le C\,h_K\|\boldsymbol{\pi}^- e_{\boldsymbol{u}}\|^2_{0,K}.
\end{aligned} \tag{52}
$$

Note that by the continuity of the projection operator $\boldsymbol{\pi}^+$ and the regularity, (44), of the dual problem we have

$$
\|\boldsymbol{\pi}^+\boldsymbol{\psi}\|_{0,K} \;\le\; C\|\boldsymbol{\psi}\|_{0,K} \;\le\; Ch_K\|\boldsymbol{\eta}\|_{0,K} \;=\; Ch_K\|\boldsymbol{\pi}^- e_{\boldsymbol{u}}\|_{0,K}. \tag{53}
$$

An estimate on T_4 now follows simply by the assumption (35). Indeed,

$$
\begin{aligned}
|T_4| &\le \|\boldsymbol{f}-\boldsymbol{f}^*\|_{0,K}\|\boldsymbol{\pi}^+\boldsymbol{\psi}\|_{0,K} \\
&\le C\,h_K^{r+1} \;\cdot\; Ch_K\|\boldsymbol{\pi}^- e_{\boldsymbol{u}}\|_{0,K} \\
&\le C\,h_K^{r+2}\|\boldsymbol{\pi}^- e_{\boldsymbol{u}}\|_{0,K}.
\end{aligned} \tag{54}
$$

To estimate T_5 we will use the inverse estimate

$$
|(\boldsymbol{\pi}^+\boldsymbol{\psi})(a^+)| \;\le\; \|\boldsymbol{\pi}^+\boldsymbol{\psi}\|_{L^\infty(K)} \;\le\; Ch_K^{-1/2}\|\boldsymbol{\pi}^+\boldsymbol{\psi}\|_{0,K}
$$

which can be found, for example, in (p. 149 of) [16]. Now, using (53), we get

$$
|(\boldsymbol{\pi}^+\boldsymbol{\psi})(a^+)| \le Ch_K^{1/2}\|\boldsymbol{\pi}^- e_{\boldsymbol{u}}\|_{0,K}. \tag{55}
$$

The estimate

$$
|T_5| \le C\,h_K^{r+3/2}\|\boldsymbol{\pi}^- e_{\boldsymbol{u}}\|_{0,K}. \tag{56}
$$

then follows from (55) and the assumption (36).

Inserting the estimates (50)–(52), (54), and (56) into (49) we obtain

$$
\begin{aligned}
\|\boldsymbol{\pi}^- e_{\boldsymbol{u}}\|^2_{0,K} &\le Ch_K^{r+2}\|\boldsymbol{\pi}^- e_{\boldsymbol{u}}\|_{0,K} + Ch_K\|\boldsymbol{\pi}^- e_{\boldsymbol{u}}\|^2_{0,K} + Ch_K^{r+3/2}\|\boldsymbol{\pi}^- e_{\boldsymbol{u}}\|_{0,K} \\
&\le Ch_K^{r+3/2}\|\boldsymbol{\pi}^- e_{\boldsymbol{u}}\|_{0,K} + Ch_K\|\boldsymbol{\pi}^- e_{\boldsymbol{u}}\|^2_{0,K}.
\end{aligned}
$$

If we assume that h_K is small enough so that $Ch_K < 1$ then

$$
\|\boldsymbol{\pi}^- e_{\boldsymbol{u}}\|^2_{0,K} \le Ch_K^{r+3/2}\|\boldsymbol{\pi}^- e_{\boldsymbol{u}}\|_{0,K}
$$

and the estimate (40) follows.

Observe that the loss of half a power of h_K is caused only by the estimate of the term T_5. In particular, if (41) is satisfied then we recover the one-full-order-superconvergent estimate (42). This finishes the proof. □

It remains to prove Lemma 4.7.

Proof. (Lemma 4.7) By the definition, (43a), of $\boldsymbol{\psi}$

$$
\begin{aligned}
(\boldsymbol{\pi}^- e_{\boldsymbol{u}},\, \boldsymbol{\eta})_K &= (\boldsymbol{\pi}^- e_{\boldsymbol{u}},\, \boldsymbol{\psi}')_K + (\boldsymbol{\pi}^- e_{\boldsymbol{u}},\, A^T\boldsymbol{\psi})_K \\
&= (\boldsymbol{\pi}^- e_{\boldsymbol{u}},\, \boldsymbol{\psi}')_K + (A\boldsymbol{\pi}^- e_{\boldsymbol{u}},\, \boldsymbol{\psi})_K
\end{aligned} \tag{57}
$$

Let us work on the first term on the right-hand side. By (47) we have

$$
(\boldsymbol{\pi}^- e_{\boldsymbol{u}},\, \boldsymbol{\psi}')_K = (\boldsymbol{\pi}^- e_{\boldsymbol{u}},\, (\boldsymbol{\xi}^+_{\boldsymbol{\psi}})')_K + (\boldsymbol{\pi}^- e_{\boldsymbol{u}},\, (\boldsymbol{\pi}^+\boldsymbol{\psi})')_K.
$$

Integrating by parts on the first term on the right-hand side and using the definition, (38), of $\boldsymbol{\pi}^+$ we get

$$\begin{aligned}(\boldsymbol{\pi}^- e_{\boldsymbol{u}},\, \boldsymbol{\psi}')_K = {} & (\boldsymbol{\pi}^- e_{\boldsymbol{u}})(b^-)\cdot \boldsymbol{\xi}^+_{\boldsymbol{\psi}}(b^-) - (\boldsymbol{\pi}^- e_{\boldsymbol{u}})(a^+)\cdot \boldsymbol{\xi}^+_{\boldsymbol{\psi}}(a^+)\\ & - ((\boldsymbol{\pi}^- e_{\boldsymbol{u}})',\, \boldsymbol{\xi}^+_{\boldsymbol{\psi}})_K + (\boldsymbol{\pi}^- e_{\boldsymbol{u}},\, (\boldsymbol{\pi}^+\boldsymbol{\psi})')_K\\ = {} & (\boldsymbol{\pi}^- e_{\boldsymbol{u}})(b^-)\cdot \boldsymbol{\xi}^+_{\boldsymbol{\psi}}(b^-) + (\boldsymbol{\pi}^- e_{\boldsymbol{u}},\, (\boldsymbol{\pi}^+\boldsymbol{\psi})')_K.\end{aligned} \tag{58}$$

Taking $\boldsymbol{v} = \boldsymbol{\pi}^+\boldsymbol{\psi}$ in (46) we get

$$\begin{aligned}(\boldsymbol{\pi}^- e_{\boldsymbol{u}},\, (\boldsymbol{\pi}^+\boldsymbol{\psi})')_K = {} & (\boldsymbol{\pi}^- e_{\boldsymbol{u}})(b^-)\cdot (\boldsymbol{\pi}^+\boldsymbol{\psi})(b^-)\\ & - (A\boldsymbol{\xi}^-_{\boldsymbol{u}},\, \boldsymbol{\pi}^+\boldsymbol{\psi})_K - (A\boldsymbol{\pi}^- e_{\boldsymbol{u}},\, \boldsymbol{\pi}^+\boldsymbol{\psi})_K\\ & - (\boldsymbol{f} - \boldsymbol{f}^*,\, \boldsymbol{\pi}^+\boldsymbol{\psi})_K - (\boldsymbol{u}_a - \boldsymbol{u}^*_a)\cdot (\boldsymbol{\pi}^+\boldsymbol{\psi})(a^+).\end{aligned}$$

Inserting this into (58) we get

$$\begin{aligned}(\boldsymbol{\pi}^- e_{\boldsymbol{u}},\, \boldsymbol{\psi}')_K = {} & - (A\boldsymbol{\xi}^-_{\boldsymbol{u}},\, \boldsymbol{\pi}^+\boldsymbol{\psi})_K - (A\boldsymbol{\pi}^- e_{\boldsymbol{u}},\, \boldsymbol{\pi}^+\boldsymbol{\psi})_K\\ & - (\boldsymbol{f} - \boldsymbol{f}^*,\, \boldsymbol{\pi}^+\boldsymbol{\psi})_K - (\boldsymbol{u}_a - \boldsymbol{u}^*_a)\cdot (\boldsymbol{\pi}^+\boldsymbol{\psi})(a^+)\end{aligned}$$

where we have used the fact that

$$\begin{aligned}&(\boldsymbol{\pi}^- e_{\boldsymbol{u}})(b^-)\cdot \boldsymbol{\xi}^+_{\boldsymbol{\psi}}(b^-) + (\boldsymbol{\pi}^- e_{\boldsymbol{u}})(b^-)\cdot (\boldsymbol{\pi}^+\boldsymbol{\psi})(b^-)\\ &\qquad = (\boldsymbol{\pi}^- e_{\boldsymbol{u}})(b^-)\cdot \boldsymbol{\psi}(b^-) \qquad \text{by (47)}\\ &\qquad = 0 \qquad \text{by (43b)}.\end{aligned}$$

Inserting the last identity into (57) we obtain

$$\begin{aligned}(\boldsymbol{\pi}^- e_{\boldsymbol{u}},\, \boldsymbol{\eta})_K = {} & - (A\boldsymbol{\xi}^-_{\boldsymbol{u}},\, \boldsymbol{\pi}^+\boldsymbol{\psi})_K - (A\boldsymbol{\pi}^- e_{\boldsymbol{u}},\, \boldsymbol{\pi}^+\boldsymbol{\psi})_K + (A\boldsymbol{\pi}^- e_{\boldsymbol{u}},\, \boldsymbol{\psi})_K\\ & - (\boldsymbol{f} - \boldsymbol{f}^*,\, \boldsymbol{\pi}^+\boldsymbol{\psi})_K - (\boldsymbol{u}_a - \boldsymbol{u}^*_a)\cdot (\boldsymbol{\pi}^+\boldsymbol{\psi})(a^+)\\ = {} & - (A\boldsymbol{\xi}^-_{\boldsymbol{u}},\, \boldsymbol{\pi}^+\boldsymbol{\psi})_K + (A\boldsymbol{\pi}^- e_{\boldsymbol{u}},\, \boldsymbol{\xi}^+_{\boldsymbol{\psi}})_K\\ & - (\boldsymbol{f} - \boldsymbol{f}^*,\, \boldsymbol{\pi}^+\boldsymbol{\psi})_K - (\boldsymbol{u}_a - \boldsymbol{u}^*_a)\cdot (\boldsymbol{\pi}^+\boldsymbol{\psi})(a^+).\end{aligned}$$

The identity (48) now follows since

$$(A\boldsymbol{\xi}^-_{\boldsymbol{u}},\, \boldsymbol{\pi}^+\boldsymbol{\psi})_K = (A\boldsymbol{\xi}^-_{\boldsymbol{u}},\, \boldsymbol{\psi})_K - (A\boldsymbol{\xi}^-_{\boldsymbol{u}},\, \boldsymbol{\xi}^+_{\boldsymbol{\psi}})_K$$

by (47). □

5. Numerical Results

In this section, we display numerical results verifying our theoretical finding. We verify numerically that the post-processing technique introduced in Section 3 results in a better approximation which converges to the exact solution with order $2k+1$ in the L^2-norm inside the elements, rather than merely at the nodes of the mesh. Finally, we show that this post-processing does not deteriorate even when the parameter d is extremely small. The fact that the original DG approximation converges with the optimal order $k+1$ in the L^2-norm and with order $2k+1$ at the nodes of the mesh have been proved and numerically verified in [5]. Thus we display only the history of convergence of the post-processed approximation.

In our experiments we consider two problems. In either problem we approximate the solution of (2)-(3) subject to homogeneous boundary conditions, namely, we take

$$w_0 = w_1 = u_0 = u_1 = \theta_0 = \theta_1 = 0.$$

In both examples we take $\kappa \equiv 1$ which corresponds to a circular arch. Although the theory has been carried out for arches with arbitrary geometry and κ can be any $L^\infty(\Omega_h)$ function which satisfies the mild restriction (11), we have to consider a circular arch since we need to compute the exact solution to the problem so that we can carry out a history of convergence study. We first employ the DG method defined by (4) with the numerical traces given by (5)-(7) which are obtained by setting

$$C_{16} = C_{25} = C_{34} = C_{43} = C_{52} = C_{61} = -1$$

for all x in $\mathcal{E}_h$, except $C_{16} = C_{25} = C_{34} = 0$ on $\partial\Omega$, and setting all the other coefficients to zero. Observe that these coefficients satisfy the conditions provided by (12)-(15), and hence the numerical traces of the DG solution are superconvergent of order $2k+1$ by Theorem 3.1. The post-processing is then computed in an element-by-element fashion as described in Steps 1–4 of Section 3. The only difference between the two problems arise from the loading of the arch. In the first example we take

$$p \equiv q \equiv 1 \qquad \text{in } \Omega$$

which corresponds to an arch which is loaded uniformly in both the transverse and tangential directions. In the second example, we take

$$p \equiv 0, \qquad q \equiv d^{-2} \qquad \text{in } \Omega$$

which corresponds to a so-called *membrane arch*. It has no tangential loads and is loaded very strongly in the transverse direction. The transverse load is taken inversely proportional to the square of the thickness of the arch due to the fact that the membrane arch is well-known to become extremely *stiff* as d converges to zero, and it becomes impossible to observe meaningful displacements unless such large transverse loads are applied. We have observed this phenomenon in our numerical experiments as well.

We display our numerical results in Tables 1 and 2. Therein k indicates the polynomial degree we used to define the DG method, and "mesh = i" means we employed a uniform mesh with 2^i elements. This also means that the post-processed approximation is a piecewise polynomial of degree at most $2k$ on each element. We display the numerical orders of convergence which are computed as follows. Let $\|\boldsymbol{e}^*(i)\|_0$ denote the $L^2(\Omega_h)$-norm of the error where a uniform mesh with 2^i elements has been employed to obtain the DG approximation and its post-processing. For brevity, rather than displaying the error for each individual unknown, we display the total error defined as

$$\|\boldsymbol{e}^*\|_0 := \left(\|e^*_w\|_0^2 + \|e^*_u\|_0^2 + \|e^*_\theta\|_0^2 + \|e^*_M\|_0^2 + \|e^*_N\|_0^2 + \|e^*_T\|_0^2\right)^{1/2}.$$

The order of convergence, r_i, at the level i is then defined as

$$r_i = \frac{\log\left(\frac{\|\boldsymbol{e}^*(i-1)\|_0}{\|\boldsymbol{e}^*(i)\|_0}\right)}{\log 2}.$$

In light of Theorem 3.4, we expect this quantity to approach $2k+1$ in the asymptotic regime. Furthermore, in order to verify that the quality of the post-processed approximation does not deteriorate as d becomes very small, we take $d = 10^{-1}$ and then decrease it down to $d = 10^{-8}$.

In Tables 1 and 2 we display our numerical results for the first and the second examples, respectively. In both cases we clearly see that the post-processed approximation converges with order $2k+1$ to the exact solution as predicted by Theorem 3.4. Moreover, these results do not deteriorate as the parameter d becomes extremely small and the convergence of the post-processed solution is robust with respect to d. This verifies the theoretically expected fact that the DG methods as well as their post-processing is free from shear and membrane locking. This is

TABLE 1. History of convergence of the post-processed DG approximation for the first problem.

		$d = 10^{-1}$		$d = 10^{-4}$		$d = 10^{-8}$	
k	mesh	$\Vert\boldsymbol{e}^*\Vert_0$	order	$\Vert\boldsymbol{e}^*\Vert_0$	order	$\Vert\boldsymbol{e}^*\Vert_0$	order
1	5	3.01E-05	3.04	3.27E-06	3.06	3.27E-06	3.06
	6	3.71E-06	3.02	4.00E-07	3.03	4.00E-07	3.03
	7	4.60E-07	3.01	4.95E-08	3.02	4.95E-08	3.02
	8	5.73E-08	3.01	6.15E-09	3.01	6.15E-09	3.01
2	5	1.72E-10	4.92	1.96E-10	4.92	1.96E-10	4.92
	6	5.57E-12	4.95	6.30E-12	4.96	6.30E-12	4.96
	7	1.78E-13	4.97	2.00E-13	4.98	2.00E-13	4.98
	8	5.62E-15	4.98	6.28E-15	4.99	6.28E-15	4.99
3	4	8.88E-14	7.19	2.43E-15	7.86	2.43E-15	7.86
	5	6.41E-16	7.12	1.08E-17	7.81	1.08E-17	7.81
	6	4.79E-18	7.06	5.20E-20	7.70	5.20E-20	7.70
	7	3.66E-20	7.03	2.84E-22	7.52	2.84E-22	7.52

TABLE 2. History of convergence of the post-processed DG approximation for the second problem.

		$d = 10^{-1}$		$d = 10^{-4}$		$d = 10^{-8}$	
k	mesh	$\Vert\boldsymbol{e}^*\Vert_0$	order	$\Vert\boldsymbol{e}^*\Vert_0$	order	$\Vert\boldsymbol{e}^*\Vert_0$	order
1	5	3.00E-03	3.04	2.14E-01	3.04	2.14E-01	3.04
	6	3.69E-04	3.02	2.64E-02	3.02	2.64E-02	3.02
	7	4.58E-05	3.01	3.28E-03	3.01	3.28E-03	3.01
	8	5.70E-06	3.01	4.08E-04	3.01	4.08E-04	3.01
2	5	1.14E-09	5.50	1.12E-07	4.51	1.12E-07	4.51
	6	8.34E-11	3.78	6.84E-09	4.04	6.84E-09	4.04
	7	3.39E-12	4.62	2.68E-10	4.67	2.68E-10	4.67
	8	1.18E-13	4.84	9.25E-12	4.86	9.25E-12	4.86
3	5	6.41E-14	7.11	4.99E-12	7.11	4.99E-12	7.11
	6	4.79E-16	7.06	3.74E-14	7.06	3.74E-14	7.06
	7	3.66E-18	7.03	2.86E-16	7.03	2.86E-16	7.03
	8	2.83E-20	7.02	2.21E-18	7.02	2.21E-18	7.02

remarkable especially for the membrane arch since the behavior of its solution is extremely sensitive to the value of the thickness of the arch, especially for small values of the parameter d.

6. Conclusion

We introduced and numerically tested a remarkably efficient and inexpensive post-processing method for the DG solutions for the Naghdi arch problem. Although the DG approximation converges with order $k + 1$ when polynomials of degree k are used, the post-processed approximation superconverges with order $2k+1$. The post-processing exploits the fact that the numerical traces of the DG method converge with order $2k+1$. This result holds independently of the thickness parameter d, which shows that the post-processing as well as the DG methods are free from shear and membrane locking.

References

[1] P. Castillo, B. Cockburn, D. Schötzau, and C. Schwab, *Optimal a priori error estimates for the hp-version of the local discontinuous Galerkin method for convection-diffusion problems*, Math. Comp. **71** (2002), 455–478.

[2] F. Celiker and B. Cockburn, *Element-by-element post-processing of discontinuous Galerkin methods for Timoshenko beams*, J. Sci. Comput. **27** (2006), no. 1–3, 177–187.

[3] ———, *Superconvergence of the numerical traces of discontinuous Galerkin and hybridized methods for convection-diffusion problems in one space dimension*, Math. Comp. **76** (2007), no. 257, 67–96.

[4] F. Celiker, B. Cockburn, and H.K. Stolarski, *Locking-free optimal discontinuous Galerkin methods for Timoshenko beams*, SIAM J. Numer. Anal. **44** (2006), no. 6, 2297–2325.

[5] F. Celiker, L. Fan, S. Zhang, and Z. Zhang, *Locking-free optimal discontinuous Galerkin methods for a Naghdi-type arch model, submitted.*

[6] B. Cockburn and B. Dong, *An analysis of the minimal dissipation local discontinuous Galerkin method for convection-diffusion problems*, J. Sci. Comput. **32** (2007), no. 2, 233–262.

[7] B. Cockburn and R. Ichikawa, *Adjoint recovery of superconvergent linear functionals from Galerkin approximations*, J. Sci. Comput. **32** (2007), no. 2, 201–232.

[8] B. Cockburn, G. Kanschat, I. Perugia, and D. Schötzau, *Superconvergence of the local discontinuous Galerkin method for elliptic problems on Cartesian grids*, SIAM J. Numer. Anal. **39** (2001), 264–285.

[9] M. Delfour, W. Hager, and F. Trochu, *Discontinuous Galerkin methods for ordinary differential equations*, Math. Comp. **36** (1981), 455–473.

[10] B. Dong and C-W. Shu, *Analysis of a local discontinuous Galerkin method for linear time-dependent fourth-order problems*, SIAM J. Numer. Anal. **47** (2009), no. 5, 3240–3268.

[11] K. Eriksson, C. Johnson, and V. Thomée, *Time discretization of parabolic problems by the discontinuous Galerkin method*, RAIRO, Anal. Numér. **19** (1985), 611–643.

[12] P. Houston, C. Schwab, and E. Süli, *Discontinuous hp-finite element methods for advection-diffusion-reaction problems*, SIAM J. Numer. Anal. **39** (2002), 2133–2163.

[13] P. Lesaint and P. A. Raviart, *On a finite element method for solving the neutron transport equation*, Mathematical aspects of finite elements in partial differential equations (C. de Boor, ed.), Academic Press, 1974, pp. 89–145.

[14] W.H. Reed and T.R. Hill, *Triangular mesh methods for the neutron transport equation*, Tech. Report LA-UR-73-479, Los Alamos Scientific Laboratory, 1973.

[15] D. Schötzau and C. Schwab, *Time discretization of parabolic problems by the hp-version of the Discontinuous Galerkin Finite Element Method*, SIAM J. Numer. Anal. **38** (2000), 837–875.

[16] C. Schwab, *p- and hp-FEM. Theory and application to solid and fluid mechanics*, Oxford University Press, New York, 1998.

[17] V. Thomée, *Galerkin Finite Element Methods for parabolic equations*, Springer Verlag, 1997.

[18] Z. Xie and Z. Zhang, *Uniform superconvergence analysis of the discontinuous Galerkin method for a singularly perturbed problem in 1-D*, Math. Comp. **79** (2010), no. 269, 35–45.

Department of Mathematics, Wayne State University, Detroit, MI 48202, USA.
E-mail: `celiker@math.wayne.edu`

Department of Mathematics, Wayne State University, Detroit, MI 48202, USA.
E-mail: `dv6986@wayne.edu`

Department of Mathematics, Wayne State University, Detroit, MI 48202, USA.
E-mail: `zzhang@math.wayne.edu`